On the Flow-Phase Diagram for Nematic Liquid Crystalline Polymer under Magnetic Field

Shufang Fu, Jing Bai

Department of Physics, Harbin Normal University, Harbin 150080, People's Republic of China

Received 19 September 2007; accepted 25 November 2007
DOI 10.1002/app.29810
Published online 14 April 2009 in Wiley InterScience (www.interscience.wiley.com).

ABSTRACT: The effect of magnetic fields on molecular configuration of liquid crystalline polymers under shear flows are numerically analyzed using the extended Doi theory in which a molecular shape parameter is admitted. The evolution equation for the probability density function of the LCP molecules is directly solved without any closure approximations. One case is considered that the magnetic field makes 45° with respect to the flow direction. We can find that the magnetic fields strongly affect on the transition among flow-orientation modes, such as tumbling, wagging, and aligning modes. And a new aligning flow-orientation mode emerges at low shear rate, which is macroscopically same as the ordinary aligning mode, but is microscopically quite different from the ordinary one. © 2009 Wiley Periodicals, Inc. J Appl Polym Sci 113: 1383–1388, 2009

Key words: polymeric liquid crystal; shear flow; Doi theory; order parameter; magnetic field

INTRODUCTION

After a development of ultrahigh strength Kevlar® fibers, which are made from liquid crystalline polyamides by DuPont in 1970, intensive researches efforts have been achieved to enhance the performance of polymeric liquid crystalline materials. The performance, such as tensile strength and modulus, are strongly depended on the orientation configuration of constitutive molecules. For example, radial and onion structures are focused on the LCP fibers. These orientation structures are mainly formed in the process, where the melt materials flow into dies, and remain in the final products. For the last few decades, many researches have been performed on the molecular orientation in the LCP flows, especially by means of theoretical and computational analysis.[1–5] One of the major advances in the theoretical LCP rheology was made by Doi in 1981, who extended the theory for semidilute polymeric fluids to that for concentrated rod-like polymeric fluids. For simple shear, the exact solutions of the Doi theory showed that at low shear rates the orientation distribution function displayed a time-periodic tumbling, followed by the steady-state or flow-aligning, where the director became stationary at high shear rates.[6] And in the region of intermediate shear rates another different dynamical phenomenon that the director oscillated about a fixed angle was predicted, called "wagging."[7] These periodic behaviors of the orientation distribution have a great effect on the final LCPs products. Therefore, there is much interest in designing and controlling the manufacturing processes to generate favorable orientation states. For low molar mass liquid crystal, usually, the particular molecular orientation adopted by molecules is fixed by means of imposing a magnetic field (or an electric field)[8–11] or employing the boundary surfaces coated with polymers or photopolymers, which can induce an orientation to the molecules. Both methods have been extensively applied in liquid crystal devices to force the special orientation of the director, such as liquid crystal displays. In contrast, although a number of simulations predict mold filling flow and fiber orientation in injection-molded parts,[12–18] few results are known about controlling the molecular orientation to obtain the uniform molecular alignment of nematic LCPs in processing. Using the continuum Leslie–Ericksen equations, Carlsson and Skarp[19] examined the stabilizing effect of an electric field on the tumbling behavior of a nematic liquid crystal. Tse and Shine[20] studied the problem of simultaneous electric and shear fields from the perspective of the two-dimensional distribution function equations following an approach similar to that of Maffettone and Marrucci.[21]

In this work, we investigate the phase transition in LCPs processing induced by application of magnetic fields and shear flow with the extended Doi theory.

Correspondence to: S. Fu (shufangfu@yahoo.com).

Contract grant sponsor: Education of Heilongjiang Province Foundation; contract grant number: 1152hq013.
Contract grant sponsor: Harbin Normal University Foundation; contract grant number: KM2006-14.

THEORY

The LCP dynamical system used in this study is subjected to a magnetic field in addition to Hydrodynamic, Brownian, and the intermolecular forces. In the Doi theory, the polymer molecules were modeled as rigid axisymmetric rods with infinite aspect ratio, and the governing equation for the orientation distribution function f, which gives the probability of finding a rod at an orientation within the solid angle $d\mathbf{u}$ of the unit vector $\mathbf{u}$, is written as:

$$\frac{\partial f}{\partial t} = \overline{D}_r \frac{\partial}{\partial \mathbf{u}} \cdot \left(\frac{\partial}{\partial \mathbf{u}} f + f \frac{\partial}{\partial \mathbf{u}} \frac{V(\mathbf{u})}{kT} \right) - \frac{\partial}{\partial \mathbf{u}} \cdot (\dot{\mathbf{u}} f), \quad (1)$$

Here, $\overline{D}_r$ denotes the average rotational diffusivity:

$$\overline{D}_r = D_s \left(1 - \frac{3}{2} \mathrm{S} : \mathrm{S} \right)^{-2}, \quad (2)$$

where D_s is the rotational diffusivity of an isotropic state, and the order parameter tensor $\mathbf{S}$, which is the second moment of the orientation distribution f, is defined by the following equation:

$$\mathrm{S} = \int_{|\mathbf{u}|=1} \left(\mathbf{uu} - \frac{\mathbf{I}}{3} \right) f dA, \quad (3)$$

Here, $\mathbf{I}$ is a unit tensor. When the effect of the magnetic field on the LCP molecules is taken into account, the mean field potential $V(\mathbf{u})$ in eq. (1) can be described as a sum of the Maier-Saupe potential and the potential due to the magnetic field, as follows:

$$V(\mathbf{u}) = -\frac{3kTU}{2} (\mathrm{S} : \mathbf{uu}) - \frac{\mu_0 \Delta\chi}{2} (\mathbf{u} \cdot \mathbf{H})^2, \quad (4)$$

where k is the Boltzmann constant, T the absolute temperature, and U the dimensionless nematic potential intensity. μ_0 is the permeability of vacuum, $\mathbf{H}$ the vector of the magnetic field, and $\Delta\chi (= \chi_{||} - \chi_{\perp})$ the magnetic anisotropy. $\dot{\mathbf{u}}$ in eq. (1) represents the rate of change of $\mathbf{u}$ by the macroscopic flow, given by

$$\dot{\mathbf{u}} = (\boldsymbol{W} + \beta \boldsymbol{A}) \cdot \mathbf{u} - \mathbf{u} \cdot (\boldsymbol{W} + \beta \boldsymbol{A}) \cdot \mathbf{uu}, \quad (5)$$

Here $\boldsymbol{W}$ and $\boldsymbol{A}$ are the corresponding rate-of-strain and velocity tensors.

And, the molecular shape parameter, β, is related to the aspect ratio, p, namely,

$$\beta = \frac{p^2 - 1}{p^2 + 1}. \quad (6)$$

For the rodlike molecules, β is chosen in the range of 0–1 with the extended Doi theory. When $\beta = 1.0$, the molecule is infinite; when $\beta = 0$, it is a sphere. The article (Ref. 22) points out that the effect of reducing the aspect ratio can be quite significant, such as from 1.0 to 0.8. If the infinite aspect ratio nematic liquid is tumbling, lowering aspect ratio will only enhance tumbling. However, a flow-aligned infinite aspect ratio liquid is transformed by lowering aspect ratio to *either* reduce the Leslie angle downward (toward the flow axis) *or* cause a tumbling transition. This effect due to aspect ratio has been explored in Ref. 23 for a variety of mesoscopic closure approximations to the Doi theory.[24]

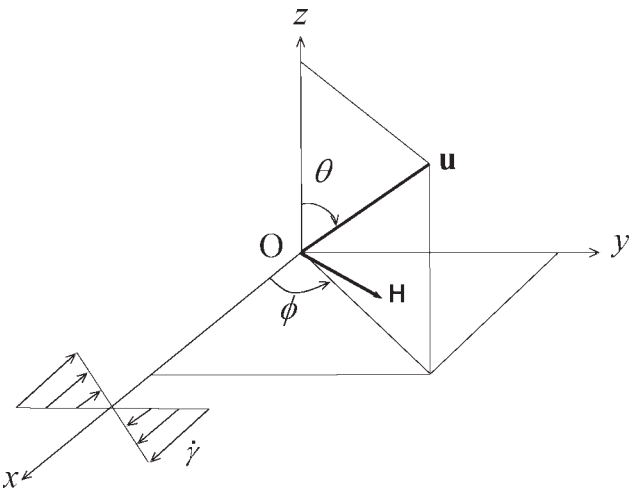

Figure 1 Geometry and coordinate systems.

NUMERICAL CALCULATION

We consider simple shear flow, as shown in Figure 1, where x-axis is the flow direction, y-axis is the direction of the velocity gradient, and z-axis is coaxial with the vorticity axis. The material is sheared with the shear rate of $\dot{\gamma}$ in the x-y plane, and the rate-of-strain and velocity tensors are given by,

$$\boldsymbol{A} = \frac{1}{2}\dot{\gamma} \begin{pmatrix} 0 & 1 & 0 \\ 1 & 0 & 0 \\ 0 & 0 & 0 \end{pmatrix}, \quad \boldsymbol{W} = \frac{1}{2}\dot{\gamma} \begin{pmatrix} 0 & 1 & 0 \\ -1 & 0 & 0 \\ 0 & 0 & 0 \end{pmatrix} \quad (7)$$

The orientation of a single molecule represented by a unit vector $\mathbf{u}$ is characterized with an azimuthal angle ϕ and a polar angle θ. The orientation distribution function f keeps symmetry with respect to the x-y plane, when the director which represents the local average of the molecular orientation always remains in the shear plane. That is,

$$f(\theta, \phi, t) = f(\pi - \theta, \phi, t), \quad (8)$$

Also, it should be mentioned here that since there is no distinction between head and tale of the model rods, the function f must has the point symmetry:

$$f(\theta, \phi, t) = f(\pi - \theta, \pi + \phi, t), \quad (9)$$

From above conditions for the distribution function f, the nonzero components of the order parameter tensor $\mathbf{S}$ are:

$$\mathrm{S} = \begin{bmatrix} S_{xx} & S_{xy} & 0 \\ S_{xy} & S_{yy} & 0 \\ 0 & 0 & S_{zz} \end{bmatrix}. \tag{10}$$

After nondimensionalization using the time scale $1/D_s$ and the magnetic force $\sqrt{2kT/\mu_0\Delta\chi}$, eq. (1) for two dimensional magnetic field [$\mathbf{H} = (H_x, H_y, 0)$] becomes

$$\begin{aligned}
\frac{\partial f}{\partial t^*} &= \left(1 - \frac{3}{2}\mathrm{S}:\mathrm{S}\right)^{-2}\left(\frac{\partial^2 f}{\partial\theta^2} + \cot\theta\frac{\partial f}{\partial\theta} + \frac{1}{\sin^2\theta}\frac{\partial^2 f}{\partial\phi^2}\right) \\
&+ 3U\left(1 - \frac{3}{2}\mathrm{S}:\mathrm{S}\right)^{-2}\{3f\left(S_{xx}\sin^2\theta\cos^2\phi + S_{yy}\sin^2\theta\sin^2\phi + S_{zz}\cos^2\theta + S_{xy}\sin^2\theta\sin 2\phi\right) \\
&- \frac{1}{2}\frac{\partial f}{\partial\theta}\sin 2\theta\left(S_{xx}\cos^2\phi + S_{yy}\sin^2\phi - S_{zz} + S_{xy}\sin 2\phi\right) + \frac{1}{2}\frac{\partial f}{\partial\phi}\left(S_{xx}\sin 2\phi - S_{yy}\sin 2\phi - 2S_{xy}\cos 2\phi\right)\} \\
&+ \left(1 - \frac{3}{2}\mathrm{S}:\mathrm{S}\right)^{-2}\left\{2f\left[H_x^{*^2}\left(3\sin^2\theta\cos^2\phi - 1\right) + H_y^{*^2}\left(3\sin^2\theta\sin^2\phi - 1\right) + 3H_x^*H_y^*\sin 2\phi\sin^2\theta\right].\right. \\
&\left. - \frac{\partial f}{\partial\theta}\left[\sin 2\theta\left(H_x^{*^2}\cos^2\phi + H_y^{*^2}\sin^2\phi + H_x^*H_y^*\sin 2\phi\right)\right] + \frac{\partial f}{\partial\phi}\left[\sin 2\phi\left(H_x^{*^2} - H_y^{*^2}\right) - 2H_x^*H_y^*\cos 2\phi\right]\right\} \\
&+ \dot\gamma^*\left\{\beta\left(\frac{3}{2}f\sin^2\theta\sin 2\phi - \frac{1}{4}\frac{\partial f}{\partial\theta}\sin 2\theta\sin 2\phi\right) + \frac{\partial f}{\partial\phi}(1 - \beta\cos 2\phi)/2\right\}
\end{aligned} \tag{11}$$

where

$$H_x^* = \frac{H_x}{\sqrt{2kT/(\mu_0\Delta\chi)}}, \tag{12}$$

$$H_y^* = \frac{H_y}{\sqrt{2kT/(\mu_0\Delta\chi)}}, \tag{13}$$

$$\dot\gamma^* = \frac{\dot\gamma}{D_s}, \tag{14}$$

$$t^* = tD_s, \tag{15}$$

The superscript "*" denotes nondimensionalized variables and parameters. Above equation is computed using the finite difference method for spatial discretization and the Crank–Nicolson method for time integration. Because of the conditions, eqs. (8) and (9), the computation area for f can be restricted in the region $0 \le \theta \le \pi/2$ and $-\pi/2 \le \phi \le \pi/2$. Boundary conditions for the function are:

$$\partial f(0, \phi, t^*)/\partial\theta = 0, \tag{16}$$

$$\partial f(\pi/2, \phi, t^*)/\partial\theta = 0, \tag{17}$$

$$f(\theta, -\pi/2, t^*) = f(\theta, \pi/2, t^*), \tag{18}$$

$$\partial f(\theta, -\pi/2, t^*)/\partial\phi = \partial f(\theta, \pi/2, t^*)/\partial\phi. \tag{19}$$

The normalization condition,

$$4\int_0^{\pi/2} d\theta \int_0^{\pi} d\phi f\sin\theta = 1, \tag{20}$$

is also required. An initial profile of the function, $f(\theta,\phi,t^* = 0)$, is derived from the Boltzmann profile with the major orientation direction along the x-axis (flow direction). The time step and the spatial mesh width are set to be $\Delta t^* = 0.005/\dot\gamma^*$ and $\Delta\theta = \Delta\phi = 3^\circ$.

RESULTS AND DISCUSSIONS

Computational parameters in eq. (11) are the dimensionless nematic potential intensity U, the dimensionless magnetic field strength H^*, and dimensionless shear rate $\dot\gamma^*$. Throughout this article, the nematic potential intensity U is set to be 5 which corresponds to the lowest order of the nematic state, to make easy to see the effect of the magnetic field on the orientation order. And $\beta = 0.9$ is considered in which the length is about 4.5 times to the diameter. In the following discussions, the computation results for the orientation distribution function will be mainly organized in terms of the major orientation angle ϕ_m and the scalar order parameter S, defined by

$$\tan 2\phi_m = \frac{2S_{xy}}{S_{xx} - S_{yy}}, \tag{21}$$

and

$$S = \sqrt{\frac{3}{2}\mathrm{S}:\mathrm{S}}. \tag{22}$$

In this section, we deal with the case that the magnetic field makes 45° with respect to the flow direction. Both of the shear flow and the magnetic field are simultaneously imposed at $t^* = 0$.

Figures 2 show the time evolutions of the major orientation angle ϕ_m and scalar order parameter S for $\dot\gamma^* = 3$ and $\mathbf{H}^* = 0$, 0.7×10^{-6}, and 1.4×10^{-6}.

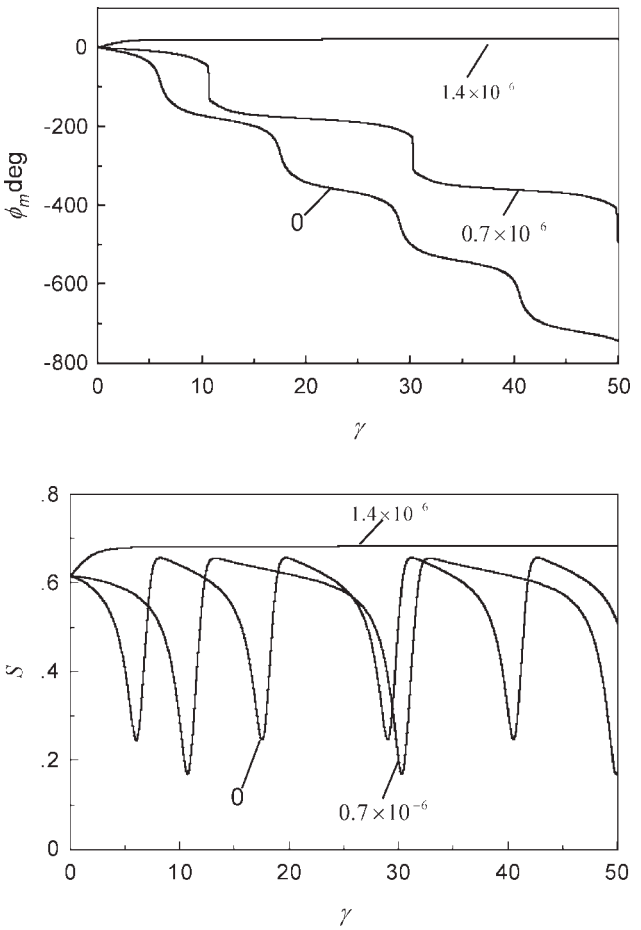

Figure 2 Transient behaviors of ϕ_m and S versus strain at $\dot{\gamma}^* = 3$ for various values of $\mathbf{H}^*$: $\mathbf{H}^* = 0$, 0.7×10^{-6}, and 1.4×10^{-6} at $\beta = 0.9$.

The horizontal axis γ represents the strain by the shear flow, which is equivalent to the dimensionless time. ϕ_m shows the typical tumbling behavior for $\mathbf{H}^* = 0$ where ϕ_m periodically decreases with γ. When the magnetic field overcomes a critical value, a kind of behavior like the aligning is represented, in which ϕ_m no longer changes with time. This new aligning is quite different from the aligning behavior at high shear rates. As known, although the major orientation angle in the aligning behavior at high shear rate remains stationary, the individual molecules continue rotating. However, the rotation of the individual molecule is suppressed by the magnetic filed in the aligning behavior at low shear rate, since the torque on the molecules by the magnetic filed overcomes the torque by the flow, which is defined by a new aligning. The behaviors of S reflect the behaviors of ϕ_m, and the steady value of S for $\mathbf{H}^* = 1.4 \times 10^{-6}$ is higher than that at the equilibrium state. Figure 3 shows the time evolutions of the major orientation angle ϕ_m and scalar order parameter S for $\dot{\gamma}^* = 5$ and $\mathbf{H}^* = 0$, 0.7×10^{-6}, and 1.4×10^{-6}. For $\mathbf{H} = 0$, the system exhibits the wagging behavior. As the magnetic field is imposed, for $\mathbf{H}^* = 0.7 \times 10^{-6}$, the period of the oscillatory behavior of ϕ_m increases and the amplitude of that decreases. Similar to the case for $\dot{\gamma}^* = 3$, the system shows the new aligning behavior above a certain critical magnetic field. Figure 4 is the time evolutions of the major orientation angle ϕ_m and scalar order parameter S for $\dot{\gamma}^* = 20$, at which the system shows the ordinary aligning behavior for all values of $\mathbf{H}^*$. The steady values of ϕ_m and S, increase with increasing $\mathbf{H}^*$.

To analyze the influence of $\mathbf{H}^*$on the scalar order parameter, the time-averaged scalar order parameter S as a function of $\mathbf{H}^*$ is shown in Figure 5. For $\dot{\gamma}^* = 20$ and 50, S increases slightly in this magnetic field strength range. However, for $\dot{\gamma}^* = 3$ and 5, S increases drastically with increasing $\mathbf{H}^*$, since the effect of the magnetic field can easily over the shear flow effect.

Next, we discuss about the effect of the magnetic field on the flow-orientation mode transition. Figure 6 represents a flow-orientation mode diagram spanned by the shear rate $\dot{\gamma}^*$ and the magnetic field strength $\mathbf{H}^*$. For the case that only the shear flow is

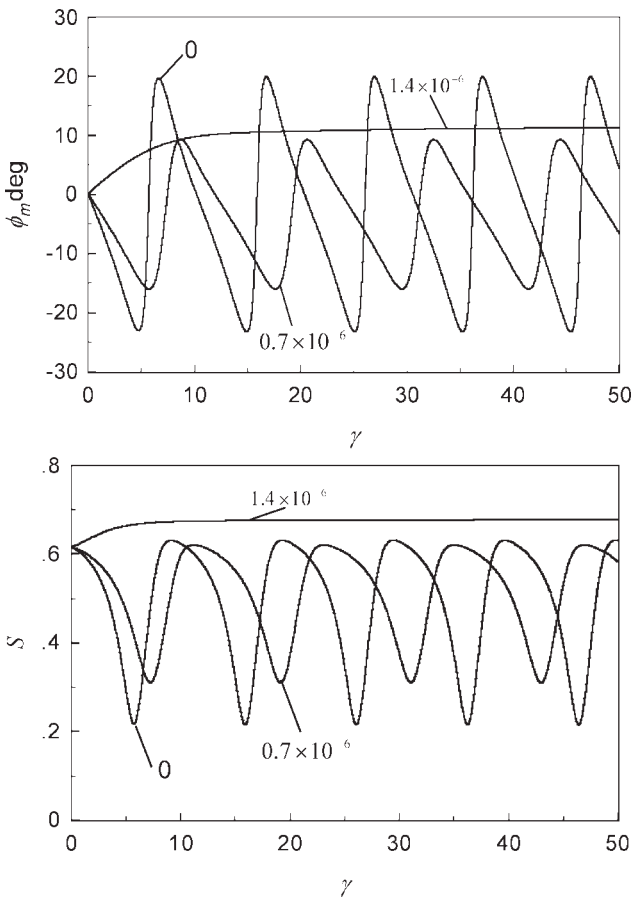

Figure 3 Transient behaviors of ϕ_m and S versus strain at $\dot{\gamma}^* = 5$ for various values of $\mathbf{H}^*$: $\mathbf{H}^* = 0$, 0.7×10^{-6}, and 1.4×10^{-6} at $\beta = 0.9$.

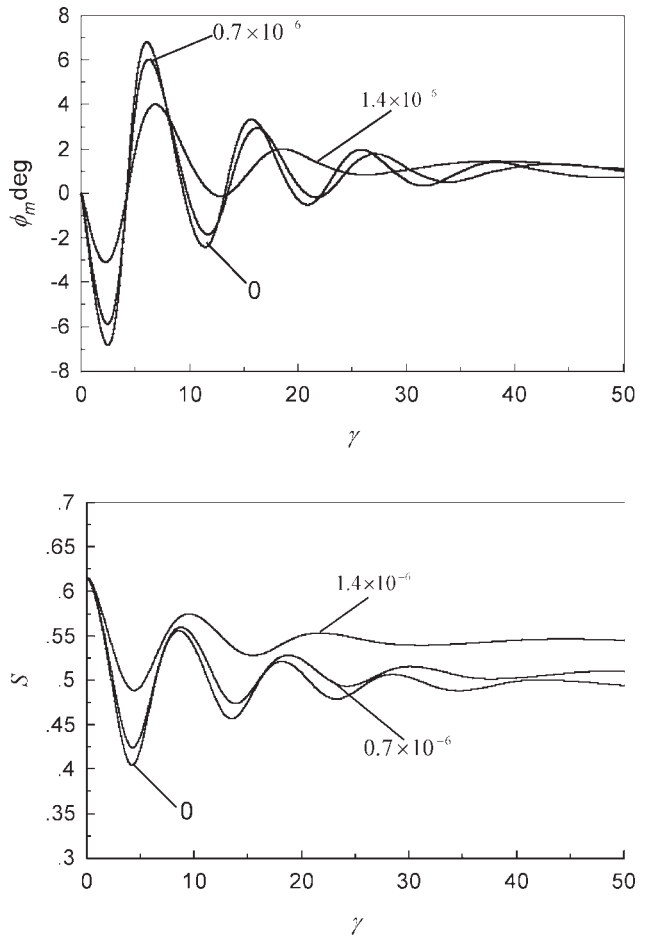

Figure 4 Transient behaviors of ϕ_m and S versus strain at $\dot{\gamma}^* = 20$ for various values of $\mathbf{H}^*$: $\mathbf{H}^* = 0$, 0.7×10^{-6}, and 1.4×10^{-6} at $\beta = 0.9$.

applied to the system (i.e., $\mathbf{H}^* = 0$), the tumbling, wagging, and aligning modes appear depending on the shear rate. At $\mathbf{H}^* = 0.71 \times 10^{-6}$, the new aligning mode regime emerges at low shear rate. This new aligning mode regime spreads toward the higher shear rate with the increase of $\mathbf{H}^*$, and takes over the whole tumbling regime at $\mathbf{H}^* = 0.99 \times 10^{-6}$. The wagging mode regime also disappears, when $\mathbf{H}^*$ is increased up to 1.31×10^{-6}. A dashed line at $\mathbf{H}^* = 1.31 \times 10^{-6}$ represents the mode transition shear rate between the new aligning mode and the ordinary aligning mode. It is expected that his transition shear rate becomes higher if $\mathbf{H}^*$ is increased further more.

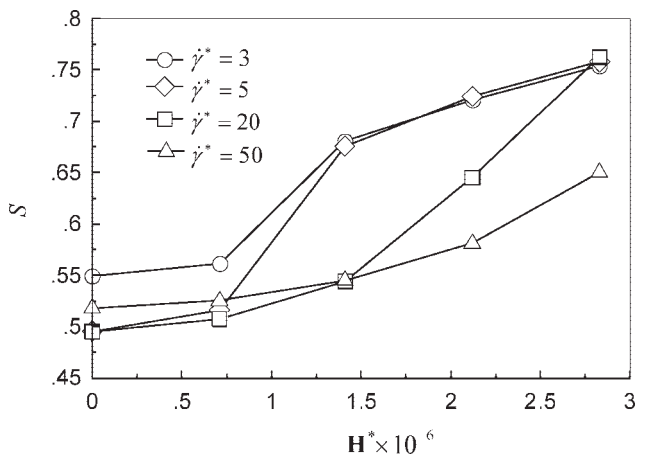

Figure 5 Effect of magnetic field on average scalar order parameter (S for various values of shear rates: $\dot{\gamma}^* = 3$, 5, 20, and 50 at $\beta = 0.9$.

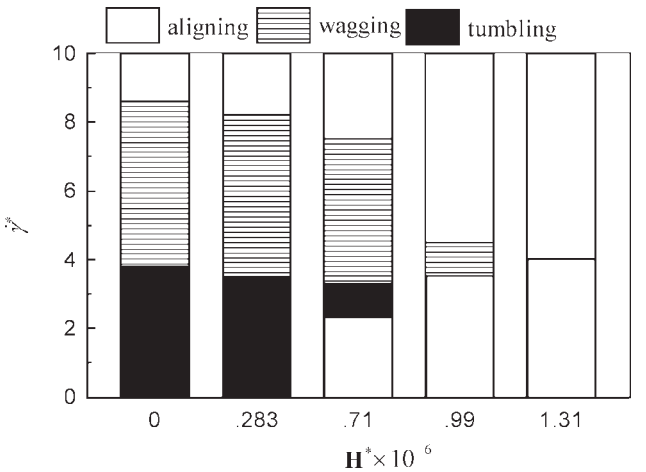

Figure 6 Critical shear rates as a function of magnetic field at $\beta = 0.9$.

CONCLUSIONS

In this article, we have simulated the evolution of LCP molecular configuration under the shear flow. In the Doi theory, the molecular configuration is represented by the probability density function of LCP molecules, in which the molecular shape parameter β is considered. The computation results are analyzed and discussed in terms of the major orientation direction, the scalar order parameter, and the flow-orientation mode transitions. When the magnetic field is imposed along the direction that makes 45° with respect to the x-axis, the scalar parameter becomes higher for entire shear rate regime. Also, the existence of the new aligning state is found at low shear rate regime in which the effect of the shear flow prevails the effect of the magnetic force, and the rotation of individual molecules is suppressed.

Through this simulation, we obtained the conclusion that the magnetic fields affect not only on the scalar order parameter and the major orientation direction, but also on the flow-orientation modes. In other words, using proper magnetic field, one can obtain the arbitrary desired molecular orientation

configurations, which enhance the functionality of the LCP materials.

The authors thank Drs. Tomohiro Tsuji and Shigeomi Chono for useful discussions.

References

1. Doi, M. J Polym Sci: Polym Phys Ed 1981, 19, 229.
2. Marrucci, G.; Greco, F. Mol Cryst Liq Cryst 1991, 17, 206.
3. Tsuji, T.; Rey, A. D. J. Non-Newtonian Fluid Mech 1997, 73, 127.
4. Tsuji, T.; Rey, A. D. Phys Rev E 1998, 57, 5609.
5. Feng, J. J.; Sgalari, G.; Leal, L. G. J Rheol 2000, 44, 1085.
6. Marrucci, G.; Maffettone, P. L. Macromolecules 1989, 22, 4076.
7. Larson, R. G. Macromolecules 1990, 23, 3983.
8. Andrews, N. C.; Edwards, B. J.; McHcgh, A. J Rheol 1995, 39, 1161.
9. Belyaev, V. V. Phys Usp 2001, 44, 255.
10. Luckhurst, G. R.; Timimi, B. A.; Nakatsuji, M.; Okumoto, K.; Sugimura, A.; Zimmermann, H. Mol Cryst Liq Cryst 2003, 398, 235.
11. Lukaschek, M.; Kothe, G. J Phys Chem 2002, 117, 4550.
12. Friedl, C.; Brouwer, R. SPE Tech Papers 1991, 37, 326.
13. Bay, R. S.; Tucker, C. L., III. Polym Compos 1992, 13, 317.
14. Bay, R. S.; Tucker, C. L., III. Polym Compos 1992, 13, 322.
15. De Frahan, H. H.; Verleye, V.; Dupret, F.; Crochet, M. J. Polym Eng Sci 1992, 32, 254.
16. Gupta, M.; Wang, K. K. Polym Compos 1993, 14, 367.
17. Henry, E.; Kjeldsen, S.; Kennedy, P. SPE Tech Papers 1994, 40, 374.
18. Randall, C.; Chiang, H. H. SPE Tech Papers 1994, 40, 397.
19. Carlsson, T.; Skarp, K. Mol Cryst Liq Cryst 1981, 78, 157.
20. Tse, K. L.; Shine, A. D. J Rheol 1995, 39, 1021.
21. Maffettone, P. L.; Marrucci, G. J Non-Newtonian Fluid Mech 1991, 38, 273.
22. Ericksen, J. L. Arch Rational Mech Anal 1960, 4, 231.
23. Forest, M. G.; Wang, Q. Rheol Acta 2003, 42, 20.
24. Forest, M. G.; Zhou, R.; Wang, Q. J Non-Newtonian Fluid Mech 2004, 116, 183.